Arab J Geosci (2017) 10: 465
https://doi.org/10.1007/s12517-017-3243-2

ORIGINAL PAPER

Provenance of sandstones from the Neoproterozoic Bombouaka Group of the Volta Basin, northeastern Ghana

C. Y. Anani[1] · A. Mahamuda[2] · D. Kwayisi[1] · D. K. Asiedu[1]

Received: 6 December 2016 / Accepted: 11 October 2017 / Published online: 30 October 2017

Abstract The provenance and tectonic setting of sandstones from the Bombouaka Group of the Voltaian Supergroup, in the northeastern part of Ghana, have been constrained from their petrography and whole-rock geochemistry. Modal analysis carried out by point-counting sandstone samples indicates that they are quartz arenites. The index of compositional variability values and SiO_2/Al_2O_3, Zr/Sc, and Th/Sc values indicates that the sediments are mature. The sandstones are depleted in CaO and Na_2O. They are, however, enriched in K_2O, Ba, and Rb relative to average Neoproterozoic upper crust. These characteristics reflect intense chemical weathering in the source region as proven by high weathering indices (i.e., CIA, PIA, and CIW). In comparison with average Neoproterozoic upper crust, the sandstones show depletion by transition metals and enrichment by high field strength elements. They generally show chondrite-normalized fractionated light rare-earth element (LREE) patterns (average La_N/Sm_N = 4.40), negative Eu anomalies (average Eu/Eu* = 0.61), and generally flat heavy rare-earth elements (HREE) (average Gd_N/Yb_N = 1.13). The sandstones have La/Sc, Th/Sc, La/Co, Th/Co, Th/Cr, and Eu/Eu* ratios similar to those of sandstones derived from felsic source. Mixing calculations using the rare-earth elements (REE) suggests 48% tonalite–trondhjemite–granodiorite and 52% granite as possible proportions for the source of the sandstones. Both the petrographic and whole-rock geochemical data point to a passive margin setting for the sandstones from the Bombouaka Group.

✉ C. Y. Anani
cyanani@ug.edu.gh

[1] Department of Earth Science, University of Ghana, Legon, Accra, Ghana

[2] Department of Earth and Environmental Sciences, University for Development Studies, Navrongo, Ghana

Keywords Geochemistry · Siliciclastic · Tectonic setting · Source rock · Modal analysis · Mature sediments

Introduction

The mineralogical and chemical compositions of siliciclastic sedimentary rocks are controlled by the composition of their source rock. Processes such as weathering, transportation, climatic conditions, and relief features affect the source rock's compositions (Armstrong-Altrin et al. 2015, 2017). These subsequently control the mineralogical and chemical compositions of siliciclastic sedimentary rocks (McLennan et al. 1990; Adel et al. 2010; Anani et al. 2013).

These may be inferred through an examination of the constituents of clastic sedimentary rocks (e.g., Condie 1993; Fedo et al. 1996; Anani et al. 2013). Studies have shown that immobile trace elements of siliciclastic sedimentary rocks such as Nb, V, Ni, Co, Sc, Y, La, and Zr are least influenced by weathering, diagenesis, and low degree of metamorphism and as such are preserved in the sedimentary rocks (Bhatia and Crook 1986; Adel et al. 2010; Armstrong-Altrin and Machain-Castillo 2016). Hence, these trace elements are suitable indicators of the source lithology, provenance, and tectonic setting (Cullers 1994; Adel et al. 2010).

The Bombouaka Group of the Voltaian Supergroup is generally divided into three formations, namely, the Tossiegou, Poubogou, and Panabako Formations, from base to top, respectively. This Group consists of medium to coarse-grained quartzitic and feldspathic sandstones at both its lower and its upper parts with the middle parts characterized by sandy shales, shales, and siltstones (Affaton 1975; Carney et al. 2010; Anani 1999; Ayite et al. 2008; Viljeon et al. 2008). The petrography, geochemistry, and provenance of the Bombouaka Group have been studied by workers such as

Anani (1999); Akah (2008); Kalsbeek et al. (2008); Carney et al. (2010), and Anani et al. (2013). For instance, Anani (1999) and Anani et al. (2013) suggested that the source of the sediments for the Kwahu Group, which is a lateral equivalent of the Bombouaka Group, could be from the weathering and erosion of Paleoproterozoic Birimian rocks. Other workers (e.g., Akah 2008; Kalsbeek et al. 2008) are of the view that the Amazonian craton could be a possible source of sediment supply for the Kwahu-Bombouaka Group. Nevertheless, most of these studies have been concentrated on the Kwahu Group in the southeastern parts of the Volta Basin. As a contribution to the ongoing researches, the petrography and whole-rock major and trace elements geochemistry of sandstones from the Bombouaka Group in the northeastern part of the Volta Basin have been analyzed to decipher their provenance and tectonic setting of the source area.

Geological setting

Regional geology

The Voltaian Supergroup that fills the Volta Basin forms part of the five main geological provinces of Ghana. It occupies the southeastern part of the West African Craton and is comparable in age to the Taoudeni basin (Fig. 1). The Voltaian Supergroup (Fig. 2) is made up of Neoproterozoic to early Paleozoic strata up to ~ 5 km thick. The strata consist of a succession of sandstones, mudstones, and few proportions of limestone (Junner and Hirst 1946; Bozhko 1969; Affaton et al. 1980; Affaton 1990; Kalsbeek et al. 2008). It covers a surface area of ~115,000 km^2. The area extends from Ghana through smaller areas in Togo, Burkina Faso, Niger, and Benin (Kalsbeek et al. 2008). Outcrops of the Voltaian Supergroup sedimentary rocks generally have shallow dips (1–2°). To the east of the basin, however, the rocks have relatively steeper dips as a result of the effect of the Pan–African orogenic event which occurred ~ 600 Ma ago (Affaton 1975; Affaton 1990). The Voltaian Supergroup is made up of three main disconformable lithostratigraphic units (Deynoux et al. 2006). They are the Kwahu-Bombouaka, Oti-Pendjari, and Tamale-Obosum Groups. The Kwahu-Bombouaka Group represents the lower lithostratigraphic unit of the basin showing epicontinental characteristics (Deynoux et al. 2006). According to Affaton (1975), the Kwahu-Bombouaka Group consists of fine to coarse-grained feldspathic sandstones with various facies of shales and siltstones intercalated with horizons of sandstones and limestones. The Oti-Pendjari Group represents the middle lithostratigraphic unit. This Group is composed of lithological assemblages of various facies of tillites, barite-bearing carbonates, and thin-bedded cherts (Carney et al. 2010). According to Deynoux et al. (2006), the Obosum Group, which is the upper lithostratigraphic unit of the Voltaian Supergroup, comprises of feldspathic sandstones as well as conglomerates deposited in the form of foreland molasses. These depositions occurred through the latter periods of uplift within the Pan-African Dahomeyide orogeny (Deynoux et al. 2006; Kalsbeek et al. 2008; Carney et al. 2010).

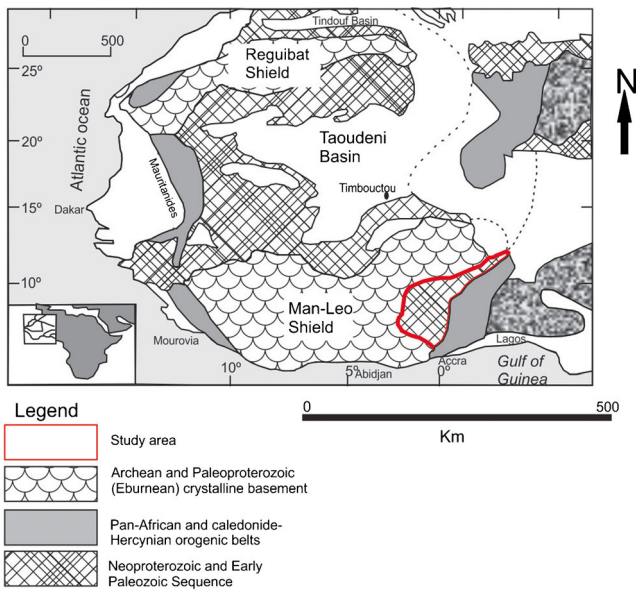

Fig. 1 Simplified geological map of the West African Craton showing the Voltaian Supergroup (after Carney et al. 2010)

The Bombouaka Group

The study area covers the northeastern margin of the Volta Basin (Fig. 2). It is underlain by the Bombouaka Group according to Affaton (1975, 1990) and Kalsbeek et al. (2008). This Group generally comprises four disconformable subdivisions (Deynoux et al. 2006), which are the Tossiegou, Poubogou, Panabako and Damongo Formations (Affaton 1975; Affaton et al. 1980; Coueffe and Vecoli 2011). The Bombouaka Group was deposited between 1000 and 600 Ma. The age of deposition was based on isotopic studies on diagenetic minerals (Clauer 1976; Bozhko et al. 1971) and detrital zircon ages (Kalsbeek and Frei 2010).

The Tossiegou Formation overlies the crystalline basement rocks belonging to the Birimian Supergroup (Fig. 2) with a major angular unconformity. It consists of conglomerates, feldspathic sandstones and coarse – grained quartzitic sandstones with characteristic ripple marks (Affaton et al. 1980; Carney et al. 2008). Overlying disconformably on the Tossiegou Formation is the Poubogou Formation (Carney et al. 2010). This formation comprises greenish-gray shales, siltstones with intercalations of fine-grained sandstones. The Poubogou Formation is about 170 m thick above the underlying

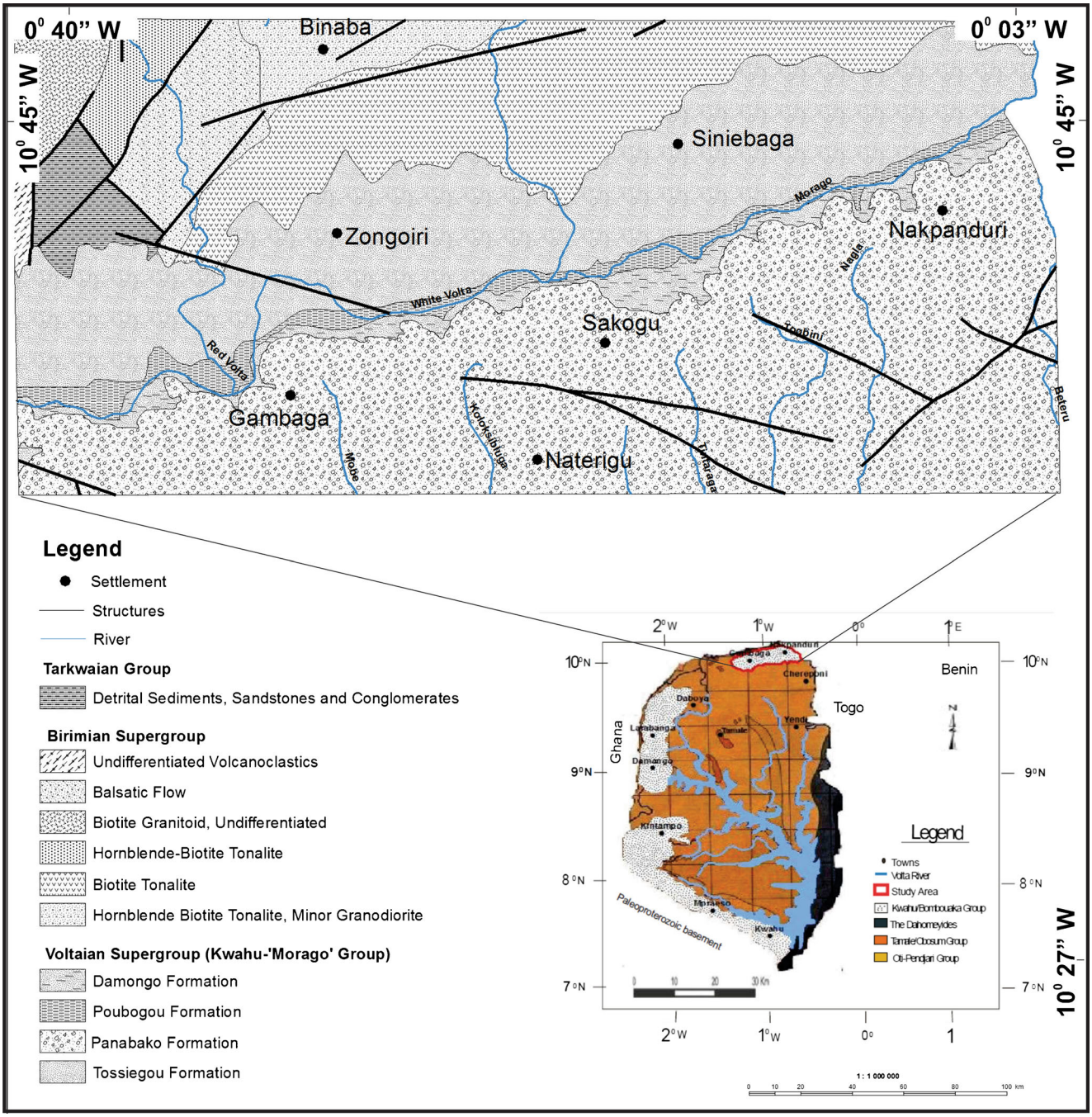

Fig. 2 Geological map showing the Bombouaka Group of the Volta Basin of Ghana (after Duodu, 2009)

Tossiegou formation in the Gambaga area (Carney et al. 2010). The Panabako Formation overlies the Poubogou Formation. It is characterized by medium to coarse-grained feldspathic sandstone and quartz arenite (Kalsbeek et al. 2008; Carney et al. 2010); finally are the flaggy, micaceous beds of the Damongo Formation. The sandstones are with ripple marks (symmetric and asymmetric) and slump structures locally (Viljeon et al. 2008). This formation is about 120 m thick and has coarser grained sandstones restricted to the upper part of the formation (Viljeon et al. 2008).

Samples and analytical methods

Twenty-six (26) thin sections were prepared for petrographic study as well as modal analysis, to estimate the modal mineralogy. The modal analysis of framework grains was carried out by point-counting using the Gazzi-Dickinson method (Dickinson 1970; Ingersoll et al. 1984). For each thin section, 300 points were counted. Whole-rock geochemical analysis of the rock samples was carried out following standard preparatory techniques. Samples were logged into the tracking

system, weighed, dried, fine-crushed each to 70% − 2 mm split off 250 g, and pulverize split to better than 85% passing 75 μm; this was done at the Analytical Laboratory System laboratory in Johannesburg, South Africa. Rare-earth element (REE) and major oxide analyses were carried out using the following methods.

The major elements were analyzed using the inductively coupled plasma-atomic emission spectroscopy (ICP-AES). First, about 0.200 g of prepared sample was fused with lithium metaborate in a furnace at 1025 °C. The resultant melt was then allowed to cool. This was then dissolved in an acid mixture consisting of nitric (HNO_3), hydrochloric (HCl), and hydrofluoric (HF) acids. The final solution was then analyzed for the major element composition using the ICP-AES with a precision better than 5%.

The base metals were also analyzed using the ICP-AES. A mixture of perchloric (HClO4), HNO3, HCl, and HF acids was used to digest a 0.25g prepared sample. The residue, after digestion, was then diluted with dilute HCl and the resultant solution was analyzed by the ICP-AES at a precision better than 7%. Results obtained were corrected for spectral interelement interferences.

The inductively coupled plasma-mass spectroscopy (ICP-MS) was used for the trace elements analysis at a precision better than 7%. The analysis was done by lithium borate fusion of prepared sample weighing 0.100 g and acid digestion in an acid mixture consisting of HNO3, HCl, and HF acids.

Results

Petrography

Modal data of representative medium-grained sandstones is shown in Table 1. The analyzed sandstones are compositionally mature (Fig. 3a–c). The framework grains consist of monocrystalline and polycrystalline quartz, K-feldspar, plagioclase, mica, rock fragments, and heavy minerals, in decreasing order of abundance. Quartz occurs as the dominant framework grain of which monocrystalline quartz (Qm) accounts for 75–96% by volume and polycrystalline quartz (Qp) for 3–14% by volume (Table 1). Monocrystalline quartz shows both non-undulose and undulose extinction (Fig. 3b). Some quartz grains have been observed with inclusions of heavy minerals such as zircons and tourmaline (Fig. 3c). The grains are subangular to well rounded (Fig. 3d). The feldspar content is low; K-feldspars dominate over plagioclase (Table 1). Most of the feldspars are altered orthoclase (Fig.3e). The lithic fragments are mainly sedimentary in origin (< 1–3%), composed of chert and shale (Fig. 3f; Table 1).

Sandstones have been classified based on the modal compositions of their matrix content and detrital framework grains. If the matrix content is less than 15%, it is an arenite and if it is greater than 15%, it is a wacke (e.g., Folk 1974; Pettijohn et al. 1972). The sandstones in the Bombouaka Group have matrix content being less than 15% and therefore are arenites (Table 1). They can be classified as quartz arenites according to the classification scheme of Pettijohn et al. 1972, (Fig. 4).

Table 1 Modal compositions of some Bombouaka Group sandstones (in vol%)

	Qm	Qp	P	K	Lv	Ls	Matrix
AM01	75.0	13.7	2.7	4.0	0.3	1.7	0.09
AM03	89.7	3.7	1.3	2.0	0.0	2.0	0.04
AM04	84.7	6.7	1.0	5.7	0.0	1.0	0.05
AM05	93.0	3.7	0.0	1.0	0.0	2.3	0.04
AM06	96.0	3.0	0.0	0.7	0.0	0.3	0.01
AM07	96.0	3.0	0.0	0.0	0.0	1.0	0.02
AM09	90.3	6.3	0.0	2.3	0.0	1.0	0.02
AM10	83.0	5.3	0.7	9.7	0.0	0.7	0.03
AM12	90.7	5.3	0.0	1.3	0.0	2.7	0.01

Categories used for sandstone point-counting: *Qp* polycrystalline quartz, *Qm* monocrystalline quartz, *Qt* total quartz (*Qt* = *Qp* + *Qm*), *P* plagioclase grains, *K* potassium feldspars, *F* total feldspar grains (*F* = *K* + *P*), *Lv* volcanic lithics, *Ls* sedimentary lithics, *L* total unstable lithic fragments (*L* = *Lv* + *Ls*), *Lt* total aphanitic rock fragments (*Lt* = *L* + *Qp*)

Geochemistry

The major and trace element concentrations are presented in Table 2. The sandstones are highly depleted in most of the major and trace elements, except SiO_2.

This could be as a result of one of the following probable causes: a deduction from a recycled sedimentary source or the removal of ferromagnesian and feldspar minerals due to extreme weathering and reworking of source area. The SiO_2 content of the Bombouaka Group sandstones ranges from ~ 87 to 98 wt%, (average 92.6 wt%). A negative correlation between SiO_2 against Al_2O_3, K_2O, and to a lesser extent MgO (Fig. 5) confirms this observation. CaO, Na_2O, P_2O_5, and to a lesser extent MgO, TiO_2 do not show any systematic variation with SiO_2 (Fig. 5). The significant correlation between Al_2O_3 and K_2O ($r = 0.81$, $n = 26$), CaO ($r = 0.84$, $n = 26$), and Na_2O ($r = 0.88$, $n = 26$) suggests that they are associated with feldspars. Also, the significant correlation between Al_2O_3 and TiO_2 ($r = 0.82$, $n = 26$), MgO ($r = 0.90$, $n = 26$), and Fe_2O_3 ($r = 0.91$, $n = 26$) suggests that these ferromagnesian elements are controlled by clay minerals and/or micas rather than non-aluminous phases such as mafic rock fragments and/or accessory oxide minerals. The ratio of K_2O/Na_2O is high (average 31.9) suggesting the dominance of potassium feldspars over plagioclase as seen in thin section (Fig. 3e; Table 1). SiO_2/Al_2O_3 has been a good indicator of sediment maturity (Pettijohn et al. 1972) with Fe_2O_3/K_2O ratio separating lithic

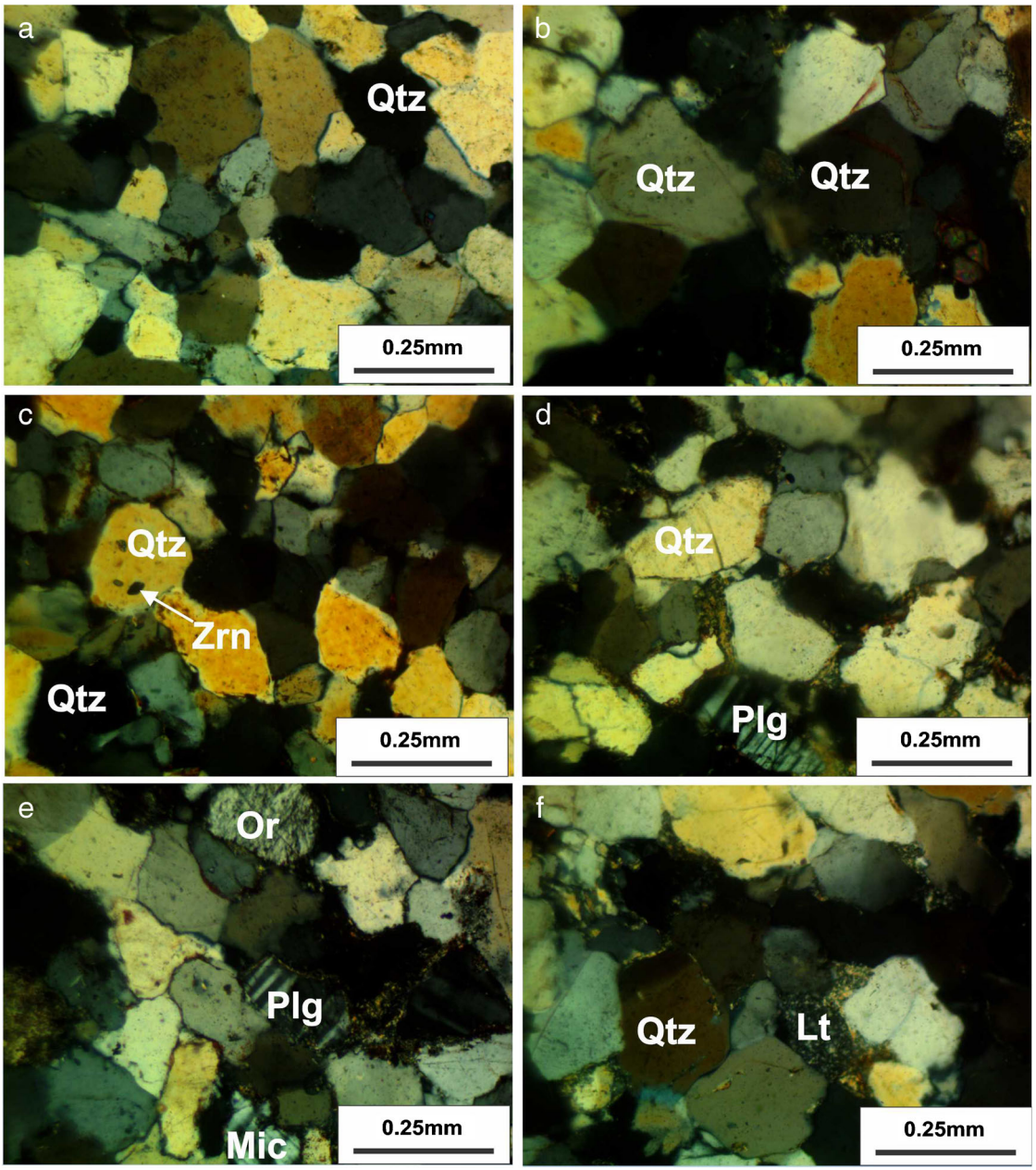

Fig. 3 Photomicrographs of sandstones from the Bombouaka Group showing **a** texturally matured grains, **b** non-undulose and undulose quartz grains, **c** zircon inclusions in quartz, **d** subrounded to well-rounded grains, **e** alteration of the feldspars, and **f** cherty lithic fragments

fragments from the potassium feldspar composition of the sandstones (Herron 1988; McLennan et al. 1993).

The sandstones from the Bombouaka Group define enriched LREE pattern and fairly flat HREE pattern with pronounced Eu negative anomalies (Eu/Eu* = 0.50–0.71; Fig. 6a). On the average upper crust normalized diagram, the studied sandstones show depletion in their major and trace element concentrations obviously due to quartz dilution effects (Fig. 6b). However, they show slight enrichment of Zr and Hf (Fig. 6b). According to Bhatia and Crook (1986) and McLennan et al. (1993), incompatible elements such as Zr and Y are mostly enriched in felsic igneous rocks relative to mafic igneous rocks and are not affected by igneous processes and generally resistant during weathering and alteration processes. The relative high amount of Zr and Y points to a felsic source of the sediments (Table 2). Moreover, the low MgO, Cr, and Ni contents of the studied samples may suggest very little or no contribution from a mafic source material. Taylor and McLennan (1985) have indicated that together with the REEs, the high field strength elements tend to be reliable identifiers of provenance composition. The Bombouaka Group sandstones show that Th, Rb, and K_2O are quite enriched while Zr displays a relative high positive anomaly (Fig. 6b).

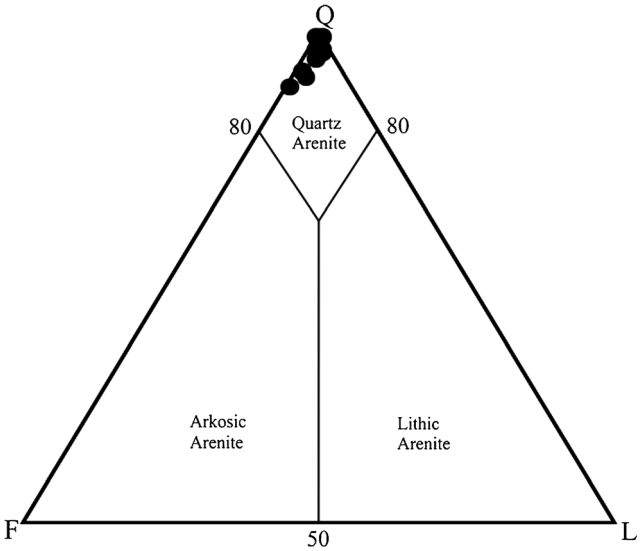

Fig. 4 Mineralogical classification of the Bombouaka Group sandstones Q, quartz; F, feldspar; and L, lithic fragments after Pettijohn et al. (1972)

Discussion

Sediment maturity

Sorting processes in clastic sedimentary rocks may be examined petrographically by evaluating the textural maturity of the sedimentary rock, using the characteristics of textures (grain sizes and shapes) and mineralogy. By their modal mineralogy, the sandstones in the Bombouaka can be classified as quartz-rich, with modal composition of quartz ranging from 88 to 99%. The sandstones are also well sorted. Therefore, on the basis of the modal mineralogy and grain sorting, the sandstones can be classified as mature sediments. However, the grains are generally not very well rounded suggesting that sedimentary recycling was not an important feature.

The SiO_2/Al_2O_3 has long been recognized as a good indicator of sediment maturity (Pettijohn et al. 1972). Increases in textural maturity of sandstones typically result in an increase in quartz content at the expense of primary clay-sized minerals, resulting in the elevation of the SiO_2/Al_2O_3 values and a decrease in the abundance of most trace elements (McLennan et al. 1993). The SiO_2/Al_2O_3 ratio has therefore been used by several workers to evaluate the textural maturity of clastic sedimentary rocks, with a high value (> 10) indicating high maturity of sediments (Armstrong-Altrin 2009, 2015). The sandstones in the Bombouaka Group have SiO_2/Al_2O_3 values between 14.7 and 79.9, suggesting that they are mature sediments.

Another test of maturity of clastic sedimentary rocks is the index of compositional variability (ICV = $(Al_2O_3 + K_2O + Na_2O + CaO + MgO + TiO_2)/Al_2O_3$; Cox et al. 1995). Immature first-cycle sedimentary rocks show index of compositional variability (ICV) values of > 1 whereas more mature sedimentary rocks show lower ICV values of < 1 (Cox et al. 1995). The sandstones of the Bombouaka Group have ICV values of < 1 suggesting that they are compositionally matured.

Th/Sc versus Zr/Sc diagram can be used to distinguish between the contrasting effects of source composition and sedimentary sorting/recycling on the composition of clastic sedimentary rocks (McLennan et al. 1993). Enrichment in zircon as a result of sorting and/or recycling would result in high Zr/Sc ratios (McLennan et al. 1993). On the Th/Sc versus Zr/Sc diagram, the sandstones of the Bombouaka Group follow a trend suggestive of heavy mineral accumulation by sediment recycling and/or sorting (Fig. 7). The observed enrichment of Zr and Hf in the sandstones relative to other trace elements (Fig. 6b) suggests zircon accumulation and therefore supports the mature and recycled nature of the sandstones (McLennan et al. 1993).

Source area weathering

The constituents of siliciclastic sedimentary rocks are controlled by chemical weathering, to a large extent. During chemical weathering, larger cations such as Rb and Ba remain fixed in the weathered residue while smaller cations such as Ca, Na, and Sr are preferentially leached due to their removal from the feldspars (Nesbitt et al., 1980; Elzien et al. 2014). These chemical trends may be transferred to the sedimentary record and may, therefore, provide a useful tool to determine the extent of chemical weathering in the source area (Fedo et al. 1996).

The chemical index of alteration (CIA; Nesbitt and Young 1982) has been used to quantitatively measure the degree of chemical weathering in the source area of sedimentary rocks (Fedo et al. 1995; Fedo et al. 1996). Intensely weathered sedimentary rocks have high CIA values (80–100), whereas incipiently weathered sedimentary rocks show CIA values in the range of 50–70 (Fedo et al. 1995). CIA values in the range of 70–75 are reported for typical shales. The CIA values of the studied samples range between 67 and 88 (avg. 75; Table 2) and may suggest moderate weathering at the source areas of the sandstones. The expected pathways for increasing degree of chemical weathering can be monitored using the Al_2O_3–(CaO* + Na_2O)–K_2O (A–CN–K) ternary diagram. The data for the Bombouaka sandstones plot on the A–K join in the A–CN–K (Fig. 8) suggesting K addition during diagenesis; weathering trends are expected to be parallel to the A–CN join. To avoid the influence of the likely remobilization of K onto the weathered residue, the plagioclase index of alteration (PIA) and chemical index of weathering (CIW) can be used Harnois, 1988; Maynard 1992; Fedo et al. 1995).

The average PIA and CIW values for the Bombouaka sandstones range from 81 to 99 and 89 to 95, respectively (Table 2), suggesting intense weathering in the source area.

Table 2 Major and trace elements concentration for the Bombouaka Group sandstones

Sample I.D	AM01	AM02	AM03	AM04	AM05	AM06	AM07	AM08	AM09	AM10	AM11	AM12	AM13	AM15
Major oxide (wt%)														
SiO2	86.5	91.6	96.7	92.1	89.7	96.3	90.5	92.4	92.8	90.1	94.7	96.5	97.8	93.2
TiO2	0.25	0.23	0.2	0.15	0.17	0.07	0.36	0.08	0.25	0.27	0.14	0.17	0.08	0.15
Al2O3	5.87	4.64	2.04	3.66	4.34	1.22	4.17	3.11	3.74	3.76	2.41	1.34	1.89	2.75
Fe2O3	1.6	1.26	0.52	1.85	2.02	1.09	1.19	0.68	0.81	1.63	0.35	0.43	0.4	0.58
MgO	0.3	0.27	0.04	0.26	0.31	0.03	0.1	0.08	0.07	0.08	0.06	0.04	0.04	0.07
CaO	0.03	0.08	0.05	0.05	0.06	0.03	0.04	0.09	0.03	0.05	0.06	0.03	0.02	0.04
Na2O	0.06	0.11	0.03	0.26	0.21	0.01	0.04	0.02	0.01	0.04	0.01	0.01	0.01	0.03
K2O	2.29	1.86	0.42	1.18	1.27	0.09	1.81	0.86	0.41	1.65	0.54	0.25	0.34	0.93
P2O5	0.03	0.03	0.01	0.02	0.02	0.01	0.01	0.02	0.01	0.04	0.06	0.01	0.02	0.01
MnO	0.01	0.03	0.01	0.04	0.04	0.01	0.01	0.01	0.01	0.01	0.01	0.01	0.01	0.01
LOI	1.91	1.47	0.95	1.42	1.69	0.75	1.1	1.3	1.55	1.02	0.95	0.57	0.76	0.86
Total	98.9	101.6	100.98	101	99.86	99.6	99.36	98.67	99.67	98.68	99.32	99.36	101.4	98.7
K2O/Na2O	38.17	16.91	14	4.54	6.05	9	45.25	43	41	41.25	54	25	34	31
K20/Al2O3	0.39	0.4	0.21	0.32	0.29	0.07	0.43	0.28	0.11	0.44	0.22	0.19	0.18	0.34
CIA	69.49	67.17	78.13	67.68	70.90	89.41	66.79	74.23	88.40	67.00	80.04	80.84	83.10	71.34
PIA	97.17	91.16	93.16	83.50	87.94	95.98	95.07	93.61	98.59	96.77	99.11	95.79	98.93	94.67
CIW	98.35	94.80	94.61	88.60	91.43	96.29	97.33	95.44	98.76	98.28	99.32	96.61	99.14	96.55
Trace elements (ppm)														
Sc	3	3	1	2	2	1	2	1	2	1	1	1	1	1
Cr	20	20	30	20	20	20	60	10	30	20	20	20	10	30
V	15	13	7	16	22	8	17	5	7	11	7	5	6	5
Co	2	2	1	5	5	2	1	1	1	1	1	1	1	1
Ni	9	6	1	9	11	2	1	1	1	2	1	1	1	1
Cu	8	6	2	2	4	5	5	2	2	3	2	5	2	2
Rb	76.3	58.8	13.8	37.1	42.5	5.2	69.5	32.8	15.6	63.4	18.3	9.7	12.6	35.7
Sr	47	45.2	16	20	21.3	18	32.9	24.9	13.9	32.4	90.2	11.8	15.8	20.1
Cs	1.21	1.03	0.35	0.6	0.74	0.2	1.12	0.74	0.6	0.85	0.4	0.27	0.3	0.56
Ba	392	355	60.7	234	268	40	297	170	35.6	305	165.5	35.4	79.2	145
Y	19.1	14.4	8.3	14.5	15.9	4.2	15	6.1	10.7	11.6	8.5	6.7	4.5	8
Zr	239	312	342	108	110	191	732	81	425	196	231	266	105	278
Hf	6.3	8.6	8.8	2.9	3	4.4	18.3	2.2	11.1	5	5.9	6.8	2.8	6.9
Nb	4.6	4.6	3.6	3.1	3.5	1.2	6.7	2	4.6	5.8	2.5	3	1.5	2.9
Ta	0.4	0.3	0.3	0.2	0.3	0.1	0.6	0.2	0.4	0.5	0.2	0.2	0.1	0.2
Th	6	6.25	5.12	3.42	3.65	1.08	8.26	2.5	6.16	5.34	3.48	3.7	1.57	2.86
U	1.75	1.79	1.28	1.46	1.6	0.52	1.3	0.47	0.97	0.89	0.97	0.84	0.64	1.24
La	25.3	17.3	10.3	13.7	14.7	11.3	16.7	14.3	20.4	17.8	28.1	8.7	10.2	10
Ce	48.8	34.2	20	35.2	37.3	24.1	33.1	24.3	30.7	34.7	51.4	17.6	18.7	18.9
Pr	5.85	3.83	2.21	3.91	4.04	2.22	3.59	2.6	3.7	3.82	5.46	1.76	2.1	1.96
Nd	22.5	14.4	8.1	16	16.3	8.1	13.7	9.3	11.8	14.9	20.1	6.5	8.1	7.9
Sm	3.35	2.63	1.54	3.06	3.16	1.12	2.77	1.57	1.93	2.77	3.39	1.09	1.55	1.41
Eu	0.58	0.49	0.26	0.57	0.46	0.24	0.55	0.31	0.34	0.47	0.58	0.17	0.29	0.26
Gd	2.94	2.2	1.37	2.82	2.49	1.04	2.64	1.26	1.73	2.01	2.38	0.87	1.21	1.29
Tb	0.47	0.41	0.18	0.37	0.42	0.13	0.4	0.18	0.32	0.36	0.33	0.19	0.17	0.18
Dy	3.11	2.52	1.31	2.37	2.78	0.83	2.73	1.18	1.76	2.35	1.74	1.14	0.94	1.25

Table 2 (continued)

Sample I.D	AM01	AM02	AM03	AM04	AM05	AM06	AM07	AM08	AM09	AM10	AM11	AM12	AM13	AM15
Ho	0.68	0.58	0.3	0.56	0.6	0.15	0.61	0.26	0.39	0.49	0.33	0.27	0.17	0.27
Er	2.08	1.59	0.95	1.51	1.66	0.45	1.74	0.72	1.23	1.3	0.92	0.78	0.53	1.01
Tm	0.31	0.25	0.14	0.23	0.25	0.06	0.3	0.08	0.18	0.2	0.12	0.11	0.08	0.14
Yb	1.97	1.69	1.1	1.57	1.89	0.55	2.01	0.77	1.51	1.58	1.09	0.89	0.56	1.1
Lu	0.3	0.26	0.16	0.23	0.3	0.08	0.35	0.1	0.23	0.23	0.14	0.13	0.08	0.17
(La/Lu)N	8.76	6.92	6.69	6.19	5.09	14.7	4.96	15.06	9.22	8.04	20.84	6.95	13.27	6.11
Eu/Eu*	0.57	0.62	0.55	0.59	0.5	0.68	0.62	0.67	0.57	0.61	0.62	0.53	0.63	0.59

Sample I.D	AM16	AM17	AM18	AM19	AM20	AM21	AM22	AM23	AM24	AM25	AM26	AM27
Major oxide (wt%)												
SiO2	95.1	94.6	90.7	92.9	96.6	93.5	97.3	95.3	96.9	93.8	94.3	91
TiO2	0.15	0.21	0.07	0.12	0.04	0.26	0.1	0.09	0.04	0.08	0.11	0.08
Al2O3	1.46	2.18	4.42	3.18	1.33	3.42	1.37	2.14	1.55	3.77	3.44	3.94
Fe2O3	0.72	0.48	0.99	0.42	0.5	0.99	0.59	0.43	0.47	0.79	0.68	0.74
MgO	0.03	0.06	0.07	0.07	0.03	0.07	0.03	0.03	0.07	0.05	0.04	0.05
CaO	0.02	0.04	0.03	0.07	0.02	0.04	0.02	0.02	0.07	0.05	0.03	0.03
Na2O	0.01	0.01	0.05	0.03	0.01	0.01	0.01	0.02	0.02	0.05	0.05	0.06
K2O	0.15	0.62	1.84	1.37	0.23	1.05	0.16	0.89	0.53	1.37	1.21	1.83
P2O5	0.01	0.01	0.01	0.04	0.01	0.02	0.01	0.01	0.02	0.01	0.02	0.02
MnO	0.01	0.01	0.01	0.01	0.02	0.01	0.01	0.01	0.01	0.01	0.01	0.01
LOI	0.77	0.94	1.25	1.01	0.61	1.18	0.73	0.73	0.71	1.19	1.01	1.07
Total	98.4	99.16	99.48	99.26	99.4	100.6	100.3	99.68	100.4	101	100.91	98.86
K2O/Na2O	15	62	36.8	45.67	23	2	16	44.5	26.5	27.4	24.2	30.5
K20/Al2O3	0.1	0.28	0.42	0.43	0.17	0.31	0.12	0.42	0.34	0.36	0.35	0.46
CIA	88.42	74.75	67.75	67.04	82.72	74.38	87.15	67.97	69.32	69.79	71.10	65.38
PIA	97.82	95.86	95.56	95.45	97.40	98.22	97.64	96.29	89.69	93.88	95.99	94.90
CIW	98.06	97.09	97.51	97.52	97.88	98.81	97.94	97.93	93.25	96.19	97.48	97.40
Trace elements (ppm)												
Sc	1	1	1	1	1	1	1	1	0.08	1	1	1
Cr	30	20	10	20	10	40	10	20	20	10	10	10
V	5	5	7	5	5	8	5	5	5	8	6	7
Co	1	1	1	1	2	1	1	1	1	1	1	1
Ni	1	1	1	1	1	2	1	1	1	1	1	1
Cu	3	2	3	3	3	2	6	2	3	3	2	2
Rb	6.6	24.6	74.3	49.1	9	42.3	8	30.6	20	50	42.7	66.8
Sr	13	21.1	29	40.9	12.3	24.7	13.5	20.4	17.1	25.1	25.4	31.8

Table 2 (continued)

Sample I.D	AM16	AM17	AM18	AM19	AM20	AM21	AM22	AM23	AM24	AM25	AM26	AM27
Cs	0.18	0.51	1.15	0.82	0.3	0.84	0.56	0.53	0.52	0.87	0.67	0.95
Ba	25.2	106.5	335	300	66.5	152.5	19.9	163	104.5	247	225	331
Y	5.7	10.3	11.7	5.6	4.2	13.3	4.8	4.2	3.1	8.3	8.2	9
Zr	247	396	81	140	43	489	157	137	59	78	114	104
Hf	6.4	10.2	2.2	3.6	1.2	12.6	4.2	3.5	1.7	2.1	3.2	2.6
Nb	2.7	3.7	1.8	2.3	0.8	4.7	1.7	1.9	1.3	1.8	2.5	1.9
Ta	0.2	0.3	0.1	0.2	0.09	0.4	0.1	0.1	0.1	0.1	0.2	0.2
Th	3.9	3.91	2.6	2.67	1.09	6.24	1.49	2.25	3.63	3.12	4.38	3.73
U	0.52	1.83	1.07	0.67	0.82	1.76	0.7	0.61	0.45	0.96	1.14	1.18
La	8.5	12.4	12.2	10.5	15.7	13	10.8	7	7	11.1	13.5	13.8
Ce	16.3	21.6	23	20.7	28.6	24.6	20.7	13.4	13.2	21.2	21.9	25.1
Pr	1.65	2.37	3.03	2.13	3.13	2.71	2.19	1.49	1.37	2.5	2.85	3.4
Nd	5.6	8.4	13.1	8.3	11	10.3	8.3	5.5	5.1	9.4	11	12.8
Sm	0.82	1.52	2.79	1.6	1.64	1.86	1.35	0.83	0.87	1.91	1.87	2.21
Eu	0.18	0.26	0.52	0.33	0.26	0.35	0.27	0.16	0.17	0.33	0.33	0.41
Gd	0.73	1.35	2.31	1.28	0.93	1.63	1.15	0.63	0.73	1.36	1.34	1.6
Tb	0.16	0.22	0.34	0.17	0.14	0.31	0.16	0.09	0.09	0.2	0.19	0.26
Dy	0.9	1.56	2.48	1.08	0.86	2.11	0.85	0.85	0.6	1.38	1.43	1.64
Ho	0.21	0.37	0.52	0.21	0.16	0.47	0.18	0.19	0.12	0.28	0.3	0.37
Er	0.7	1.27	1.71	0.58	0.51	1.53	0.57	0.47	0.37	0.87	0.96	1.03
Tm	0.1	0.19	0.29	0.11	0.07	0.21	0.08	0.07	0.04	0.15	0.15	0.16
Yb	0.75	1.27	1.72	0.79	0.4	1.48	0.68	0.56	0.36	1.04	0.97	1.13
Lu	0.12	0.21	0.27	0.12	0.08	0.25	0.13	0.08	0.06	0.13	0.15	0.16
(La/Lu)N	7.35	6.13	4.69	9.08	20.42	5.4	8.62	9.1	12.14	8.86	9.35	8.96
Eu/Eu*	0.71	0.55	0.63	0.71	0.64	0.61	0.66	0.68	0.65	0.63	0.64	0.67

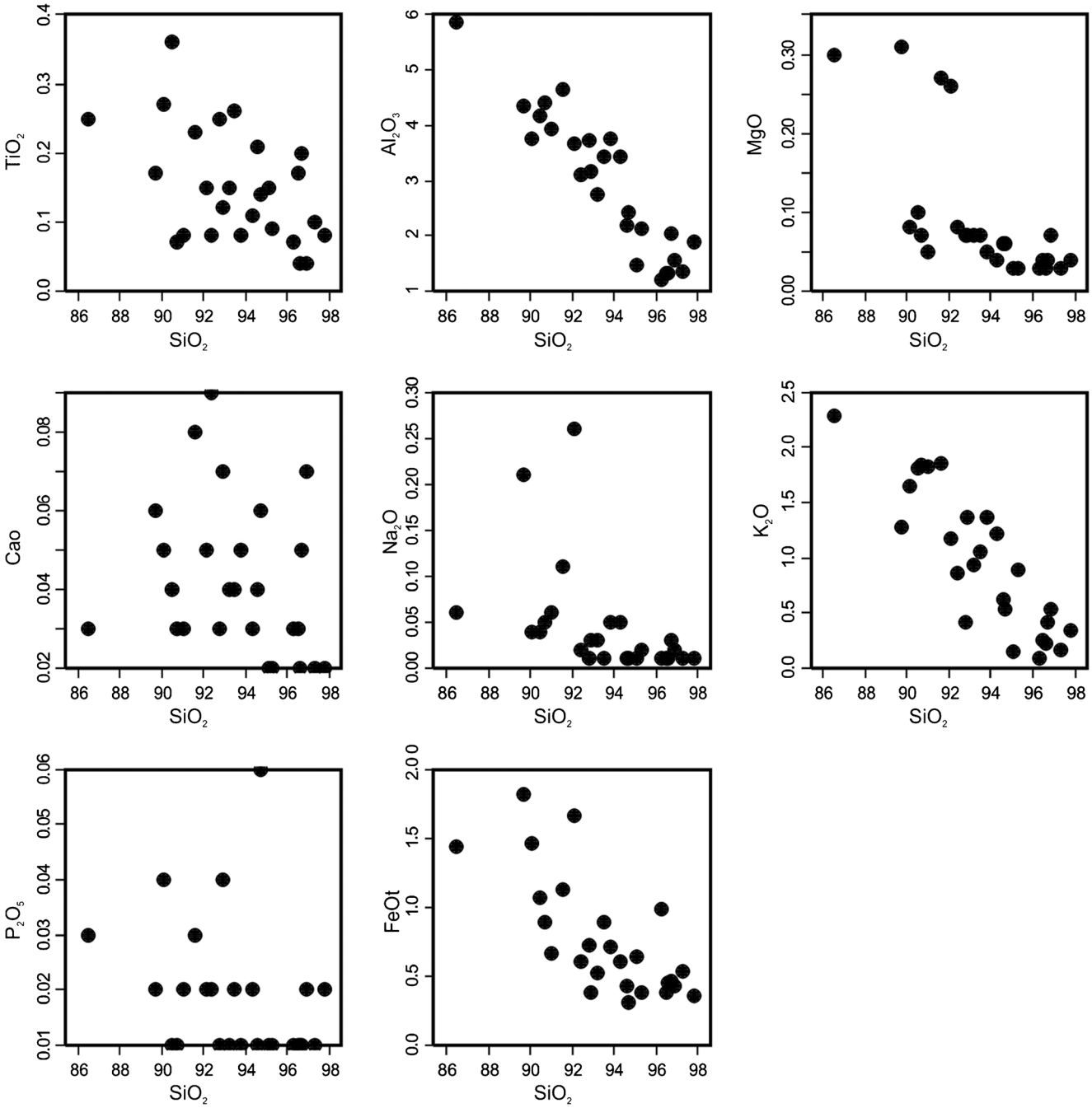

Fig. 5 Harker diagram of the sandstones of the Bombouaka Group sandstones

Source rock composition

The dominance of quartz grains over the other types of framework grains in the sandstones and the high proportion of monocrystalline quartz grains over polycrystalline quartz grains suggest derivation of the sandstones from granitic and/or gneissic source (Tortosa et al. 1991). Most of the monocrystalline quartz grains show non-undulose quartz grains and suggest derivation from plutonic rocks (Basu et al. 1975). However, the occurrence of sedimentary rock fragments and strained polycrystalline quartz with sutured contacts between sub-grains suggests a minor contribution from sedimentary and metamorphic sources, respectively. The presence of quartz grains with inclusions of heavy minerals also supports granitic sources (Morton et al. 1993). This interpretation agrees with earlier work carried out by Anani (1999) as well as Coueffe and Vecoli (2011) on the laterally equivalent Kwahu Group. They suggested that the source rocks are mainly of felsic plutonic origin with associated metasediments.

Immobile trace elements such as Nb, Zr, Hf, and Th are enriched in felsic rocks, whereas Co, Cr, Ni, and Sc are more concentrated in mafic rocks (Taylor and McLennan 1985). In

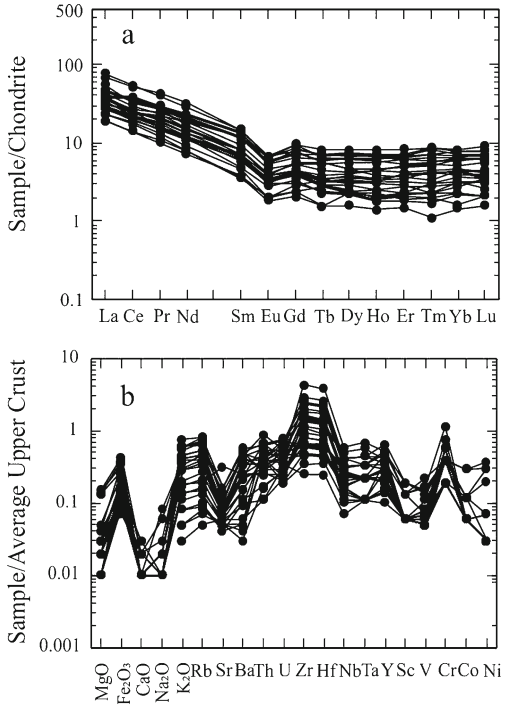

Fig. 6 **a** Chondrite-normalized REE pattern of the sandstones of the Bombouaka Group. Normalized values of chondrite (Boynton 1984) and **b** a plot of sandstone samples from the Bombouaka Group normalized against average juvenile upper crust (1.6–0.8 Ga), (values from Condie (1993)

addition, felsic igneous rocks contain negative Eu anomalies (Eu/Eu*) whereas mafic igneous rocks contain little or no Eu anomalies (Cullers et al. 1987; Cullers 2000). Therefore, trace element proportions like Th/Cr, Th/Sc, La/Sc, La/Co, and Th/Co, as well as Eu/Eu* are sensitive indicators of source rock compositions (Cullers 2000). When compared to range of Th/Cr, Th/Sc, La/Sc, La/Co, and Th/Co, as well as Eu/Eu* in sandstones from granitoids and mafic sources, the sandstones of the Bombouaka Group show elemental ratios comparable

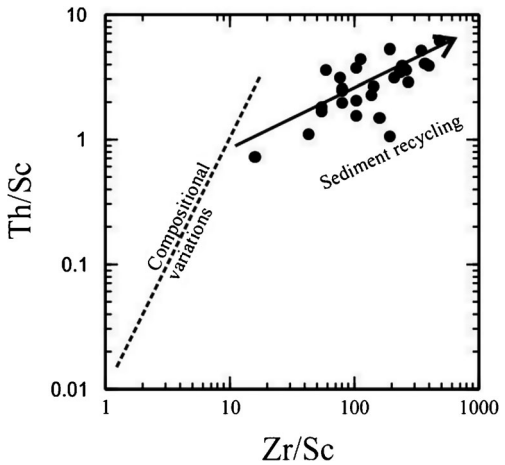

Fig. 7 Plot of Th/Sc versus Zr/Sc for sandstones of the Bombouaka Group (after McLennan et al. 1993)

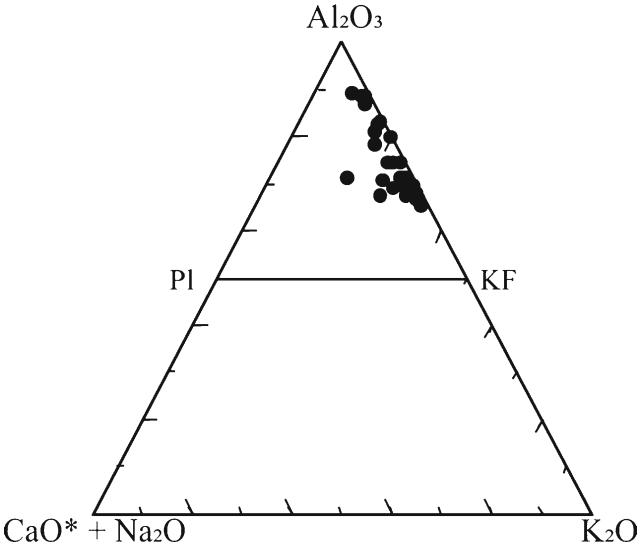

Fig. 8 A–CN–K ternary diagram showing the weathering conditions of the sandstones of the studied area (after Fedo et al. 1995)

to sandstones derived from silicic sources (Table 3). In addition, on the upper crust normalized plot, the sandstones of the Bombouaka Group display enrichment in Zr, Hf, and Th, and a depletion in Co, Cr, Ni, and Sc (Fig. 6b) suggesting predominantly felsic sources for the sandstones. It appears from the above that the sandstones of the Bombouaka Group were derived mostly from granitoid sources.

With the identification of predominantly granitic source components for the sandstones of the Bombouaka Group, it is possible to quantitatively constrain the relative contribution of granite and tonalite–trondhjemite–granodiorite (TTG) to the composition of the sandstones. Based on the average REE composition of the Bombouaka Group sandstones, mixing calculations were carried out to estimate the relative contribution of these two endmembers required to generate the Bombouaka Group sandstones. Because Neoproterozoic granitic rocks are not available in Ghana, the REE data endmembers were taken from average late Proterozoic

Table 3 Range of elemental ratios of sandstones from the Bombouaka Group compared to range of ratios in sandstones derived from granitoids and basic rocks

	Bombouaka Group[a] $N = 26$	Silicic sources[b]	Basic sources[b]
Th/Sc	0.73–6.24	0.84–20.5	0.05–0.22
La/Sc	2.07–28.1	2.50–16.3	0.43–0.86
La/Co	1.46–28.1	1.80–13.8	0.14–0.38
Th/Cr	0.05–0.44	0.13–2.70	0.02–0.05
Th/Co	0.52–8.26	0.67–19.4	0.04–1.40
Eu/Eu*	0.50–0.71	0.40–0.94	0.71–0.95

[a] Study area

[b] From Cullers (2000)

Table 4 Mixing calculation results for the Bombouaka Group sandstones

	Average Bombouaka Group Sandstone		Mixing end members				Mixing results	
			Granite (G)		TTG		52% G, 48% TTG	
	ppm	*N*	ppm	*N*	ppm	*N*	ppm	*N*
La	14.04	37.95	48.00	129.73	26.00	70.27	37.44	101.19
Ce	27.07	28.29	115.00	120.17	45.00	47.02	81.40	85.06
Nd	11.69	16.44	54.00	75.95	20.00	28.13	37.68	53.00
Sm	2.14	9.26	8.70	37.66	4.50	19.48	6.68	28.94
Eu	0.39	4.50	1.00	11.49	1.30	14.94	1.14	13.15
Gd	1.79	5.85	8.17	26.70	4.09	13.37	6.21	20.30
Tb	0.28	4.81	1.28	22.07	0.63	10.86	0.97	16.69
Yb	1.21	4.89	3.50	14.11	1.50	6.05	2.54	10.24
Lu	0.19	4.87	0.58	15.22	0.23	6.04	0.41	10.81
La_N/Sm_N		4.10		3.44		3.61		3.50
Gd_N/Yb_N		1.19		1.89		2.21		1.98
La_N/Yb_N		7.75		9.19		11.62		9.88
Eu*/Eu		0.61		0.36		0.93		0.63

N normalized values, *TTG* tonalite–trondjemite–granodiorite

chemical compositions of granite and TTG reported by Condie (1993). The mixing calculations were set in a matrix form as:

$$\begin{bmatrix} \frac{Eu*}{Eu} \\ \frac{La}{Yb} \end{bmatrix} = \begin{bmatrix} 0.36 & 0.93 \\ 9.19 & 11.62 \end{bmatrix} \begin{bmatrix} x \\ y \end{bmatrix} = \begin{bmatrix} 0.61 \\ 7.75 \end{bmatrix}$$

where:

x granite
y TTG
La/Yb is chondrite normalized

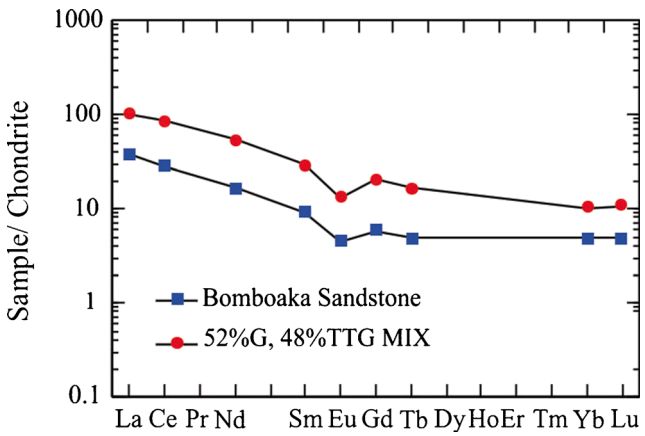

Fig. 9 Results from mixing calculations for the REEs plotted with average sandstones of the Bombouaka Group. See Table 4 for mixing parameters

The results of the mixing calculations (Table 4; Fig. 9) show that the studied Bombouaka sandstones can be represented by a mixture of 51.7% granite and 48.3% TTG.

Source area locations

The source rocks for the Bombouaka Group sandstones have been modeled as 48% TTG and 52% granite. Such granitoid rocks occur in the Paleoproterozoic Birimian basement underlying the Volta basin, and therefore, it is possible that the sandstones were derived, or at least in part, from this basement. This interpretation is supported by the occurrence of 1800–2200 Ma zircons in sandstones of laterally equivalent Kwahu Group (Kalsbeek et al. 2008; Akah 2008) and Sm–Nd whole-rock model ages of Bombouaka Group that typically fall between 1.85 and 2.28 Ga (Kalsbeek and Frei 2010). Previous works have also pointed to the Birimian rocks as source of the Bombouaka and Kwahu Groups based on structural, petrographic, and sedimentological evidences (Anani 1999; Coueffe and Vecoli 2011). Granitoids occur in both the Paleoproterozoic Birimian volcanic (greenstone) belts and the sedimentary basins. However, the granitoids in the volcanic belts are typically TTG in composition and lack the pronounced negative europium anomalies of typically less than 0.7 observed in the Bombouaka Group sandstones (this study; Kalsbeek and Frei 2009). It is therefore unlikely that the granitoids from the Birimian volcanic belts are a major contributor of detritus for the Bombouaka Group sandstones. The granitoids from the

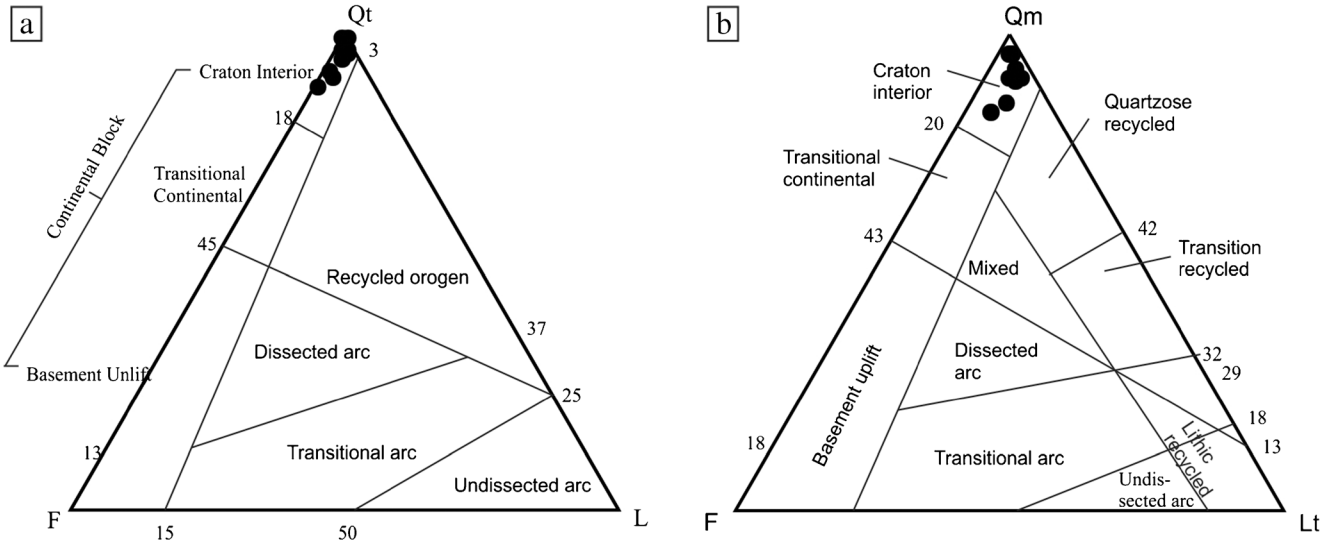

Fig. 10 Tectono-provenance discrimination diagrams (after Dickinson et al., 1983)

Birimian metasedimentary rocks are the most likely candidates.

Zircon populations dated between ~ 2000 and 1000 Ma have been reported in the sandstones of the laterally equivalent Kwahu Group (Kalsbeek et al. 2008). The West African Craton lacks Mesoproterozoic rocks with ages between 1600 and 1000 Ma and, therefore, an Amazonian source for the Kwahu-Bombouaka Group as proposed by Kalsbeek et al. (2008) may also be a possibility.

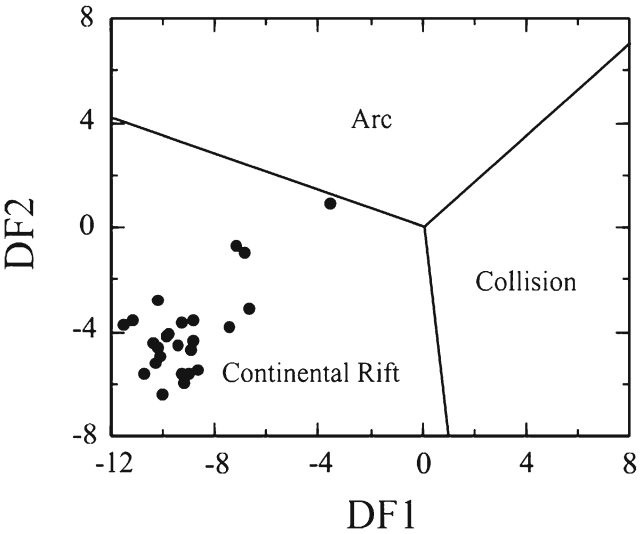

Fig. 11 Discriminant-function multi-dimensional diagram for high-silica clastic sediments (Verma and Armstrong-Altrin 2013). The subscript $_{m1}$ in DF1 and DF2 represents the high-silica diagram based on $\log_e$ ratios of major elements. The discriminant function equations are: $DF1_{(Arc\text{-}Rift\text{-}Col)}$ ml $= (-0.263 \times In(TiO_2/SiO_2)_{adj}) + (0.604 \times In(Al_2O_3/SiO_2)_{adj}) + (1.725 \times In(Fe_2O_3^t/SiO_2)_{adj}) + (0.660 \times In(MnO/SiO_2)_{adj}) + (2.191 \times In(MgO/SiO_2)_{adj}) + (0.144 \times In(CaO/SiO_2)_{adj}) + (-1.304 \times In(Na_2O/SiO_2)_{adj}) + (0.054 \times In(K_2O/SiO_2)_{adj}) + (-0330 \times In(P_2O_5/SiO_2)_{adj}) + 1.588$. $DF2_{(Arc\text{-}Rift\text{-}Col)}$ ml $= (-1.196 \times In(TiO_2/SiO_2)_{adj}) + (1.604 \times In(Al_2O_3/SiO_2)_{adj}) + (0.303 \times In(Fe_2O_3^t/SiO_2)_{adj}) + (0.436 \times In(MnO/SiO_2)_{adj}) + (0.838 \times In(MgO/SiO_2)_{adj}) + (-0.407 \times In(CaO/SiO_2)_{adj}) + (-1.021 \times In(Na_2O/SiO_2)_{adj}) + (-1.706 \times In(K_2O/SiO_2)_{adj}) + (-0.126 \times In(P_2O_5/SiO_2)_{adj}) + 1.068$.

Tectonic setting

The composition of sediment is controlled by the composition of its source rocks which in turn is controlled by the tectonic setting. Hence, it is possible to classify clastic sediments on the basis of the tectonic setting of their source terrain (Verma and Armstrong-Altrin 2016).

Dickinson et al. (1983) asserted that provenance and tectonic setting of sandstones can be deciphered by considering their Q–F–L and Qm–F–Lt compositional diagrams. The sandstones from the Bombouaka Group plot in the craton interior field on the Q–F–L and Qm–F–Lt diagrams (Fig. 10a, b).

Discriminant function-based major-element diagrams have been developed for the tectonic discrimination of siliciclastic sedimentary rocks (e.g., Bhatia 1983; Verma and Armstrong-Altrin 2013). Plotting our data into the relevant discriminant diagram of Verma and Armstrong-Altrin (2013) shows that the Bombouaka Group sandstones were deposited in a continental rift setting (Fig. 11). Continental rifts result from extensional processes within continents and include passive margins (Verma and Armstrong-Altrin 2013).

Previous investigations are generally in agreement with the passive margin interpretation for the Bombouaka Group in this study. Carney et al. (2010) on petrographic and sedimentological evidence suggested a passive margin setting for the Bombouaka Group.

Conclusions

1. The sandstones of the Bombouaka Group can be classified as quartz arenites on the basis of modal analysis of framework grains.
2. The sandstones were derived from weathered silica-rich source materials, most probably from granitoids. Mixing calculations suggest the proportion of source components could be 48% TTG and 52% granite.
3. Petrofacies analyses of the sandstones suggest a craton interior setting and geochemical analysis indicates a dominantly felsic source input from a passive margin.
4. PIA and CIW values of the Bombouaka Group sandstones indicate that the source region encountered extremely high chemical weathering.
5. The source region was most likely the granitic rocks of the Paleoproterozoic Birimian sedimentary basins and/or Mesoproterozoic granitic terranes exposed in the Amazonian craton to the north of the Volta basin.

Acknowledgements Funding for this work was received from the Department of Earth Science Capacity Building Project, University of Ghana.

References

Adel N, Mahdi J, Reza M (2010) Provenance and tectonic setting of upper Devonian sandstones from Ilanqareh Formation (NW Iran). Revista Mexicana de Ciencias Geológicas 27(3):545–561

Affaton P (1975) Etude géologique et structurale du Nord-Ouest Dahomey, du Nord Togo et du Sud-Est de la Haute-Volta, vol 10. Laboratoire Sciences de la Terre (B), Marseille, France, p 201

Affaton P (1990) Le bassin des Volta (Afrique de l'Ouest): une marge passive, d'âge protérozoïque supérieur, tectonisée au Panafrican (600±50 Ma). Editions ORSTOM, Collection Etudes et Thèses Paris, p 500

Affaton P, Sougy J, Trompette R (1980) The tectono-stratigraphic relationships between the upper Precambrian and lower Paleozoic Volta Basin and the Pan–African Dahomeyideorogenic belt West Africa. Am J of Sci 280:240–248

Akah A K (2008) Detrital zircon geochronology by LA-ICP-MS: Voltaian sediments from the Gambaga and Kintampo massifs. Voltaian Basin Workshop Excursion: 55–56

Anani C (1999) Sandstone petrology and provenance of the Neoproterozoic Voltaian Group in the southeastern Voltaian Basin, Ghana. Sed Geol 128:83–98

Anani C, Moradeyo M, Atta-Peters D, Kutu J, Asiedu D, Boamah D (2013) Geochemistry and provenance of sandstones from Anyaboni and surrounding areas in the Voltaian basin, Ghana. Int Res J Geol and Mining 3(6):206–212

Armstrong-Altrin JS (2009) Provenance of sands from Cazones, Acapulco, and Bahía Kino beaches, Mexico. Rev Mex Cien Geol 26(3):764–782

Armstrong-Altrin JS (2015) Evaluation of two multi-dimensional discrimination diagrams from beach and deep sea sediments from the Gulf of Mexico and their application to Precambrian clastic sedimentary rocks. Int Geo Review 57:1446–1461

Armstrong-Altrin JS, Machain-Castillo ML (2016) Mineralogy, geochemistry, and radiocarbon ages of deep sea sediments from the Gulf of Mexico, Mexico. J South Ame E Sci 71:182–200

Armstrong-Altrin JS, Nagarajan R, Balaram V, Natalhy-Pineda O (2015) Petrography and geochemistry of sands from the Chachalacas and Veracruz beach areas, western Gulf of Mexico, Mexico: constraints on provenance and tectonic setting. J South Ame E Sci 64:199–216

Armstrong-Altrin JS, Lee YI, Kasper-Zubillaga JJ, Trejo-Ramírez E (2017) Mineralogy and geochemistry of sands along the Manzanillo and El Carrizal beach areas, southern Mexico: implications for palaeoweathering, provenance, and tectonic setting. Geol J 52(4):559–582

Ayite A, Awua F, Kalvig P (2008) Lithostratigraphy of the Gambaga massif. Voltaian Basin Workshop Excursion:41–44

Basu A, Steven W, Young LJ, Sutter W, Calvin J, Mack GH (1975) Re-evaluation of the use of undulatory extinction and polycrystallinity in detrital quartz for provenance interpretation. J Sediment Petrol 45: 873–872

Bhatia MR (1983) Plate tectonics and geochemical composition of sandstones. J Geol 92:181–193

Bhatia MR, Crook AW (1986) Trace element characteristics of greywackes and tectonic setting discrimination of sedimentary basins. Contrib Mineral Petrol 92:181–193

Boynton WV (1984) Cosmochemistry of the rare earth elements: meteorite studies. Henderson, P., Eds., Rare Earth Element Geochemistry. Elsev Amster, In, pp 63–114

Bozhko N A (1969) Stratistraphy and tectonics of the Voltaian Basin. Annales de la Faculte des Sciences de l'University de Clermont Ferrand 41, Geol et Mineral

Bozhko NA, Kasakov GA, Trofimov DM, Knorre KG, Gatinski YUA (1971) New absolute dating of west African glauconites. Dokl Akad Nauk SSSR 198:138–139

Carney J, Jordan C, Thomas C, McDonnell P (2008) A revised lithostratigraphy and geological map for the Volta Basin, derived from image interpretation and field mapping. Voltaian Basin Workshop Excursion: 87–90

Carney JN, Jordan CJ, Thomas CW, Jordan DJ, Kemp SJ, Duodo JA (2010) Lithostratigraphy, sedimentation and evolution of the Volta Basin in Ghana. Precam Res 183:701–724

Clauer N (1976) Géochimie isotipique du strontium des milieux sédimentaires. Application à la géochronologie de la couverture du craton Ouest-Africain. Thèse Sc. Strasbourg, Sc. Géol. Mem., 45. Strasbourg, p 256

Condie KC (1993) Chemical composition and evolution of the upper continental crust: contrasting results from surface samples and shales. Chem Geol 104:1–37

Coueffe R, Vecoli M (2011) New sedimentological and biostratigraphic data in the Kwahu Group (Meso- to Neo-Proterozoic), southern margin of the Volta Basin, Ghana: stratigraphic constraints and implications on regional lithostratigraphic correlations. Precam Res 189:155–175

Cox R, Lowe DR, Cullers RD (1995) The influence of sediment recycling and basement composition on evolution of mudrock chemistry in the southwestern United States. Geochim Cosmochim Acta 59: 2919–2940

Cullers RL (1994) The controls on the major and trace element variation of shales, siltstones, and sandstones of Pennsylvanian-Permian age from uplifted continental blocks in Colorado to platform sediment in Kansas, USA. Geochim Cosmochim Acta 58(22):4955–4972

Cullers RL (2000) The geochemistry of shales, siltstones and sandstones of Pennsylvanian Permian age. Colorado, USA: implications for provenance and metamorphic studies: Lithos 51:181–203

Cullers RL, Barrett T, Carlson R, Robinson B (1987) Rare-earth element and mineralogic changes in Holocene soil and stream sediment: a case study in the wet mountains region, Colorado, USA. Chem Geol 63:275–297

Deynoux M, Affaton A, Trompette R, Villeneuve M (2006) Pan-African evolution and glacial events registered in Neoproterozoic to Cambrian cratonic and foreland basins of West African. J Afr Earth Sci 46:397–426

Dickinson WR (1970) Interpreting detrital modes of greywacke and arkose. J Sediment Petrol 40:695–707

Dickinson WR, Beard S, Brakenbridge F, Erjavec J, Ferguson R, Inman K, Knepp R, Lindberg P, Ryberg P (1983) Provenance of North American Phanerozoic sandstones in relation to tectonic setting. Geol Soc of Am Bull 64:233–235

Duodu, J.A., 2009, Ghana National Geological map Project (sheet 1:1000 000). Geological survey Department of Ghana p 1

Elzien SM, Farah AA, Elzien AB, Mohamed AA, Al-Imam OAO, Hussein AH, Khalid MK, Hamed BO, Elzien AB (2014) Geochemistry of Merkhiyat sandstones, Omdurman Formation, Sudan: implication of depositional environment, provenance and tectonic setting. Int J Geol Agri Environ Sci 2(3):10–15

Fedo CM, Nesbitt HW, Young GM (1995) Unraveling the effects of potassium metasomatism in sedimentary rocks and paleosols, with implications for paleoweathering conditions and provenance. Geol 23:921–924

Fedo CM, Eriksson KA, Krogstad EJ (1996) Geochemistry of shales from the Archean (3.0 Ga) Buhwa Greenstone Belt, Zimbabwe: implications for provenance and source-area weathering. Geochim Cosmochim Acta 60:1751–1763

Folk RL (1974) Petrology of sedimentary rocks, 2nd edn. Hemphill Press, Austin, TX

Harnois L (1988) The CIW index: a new chemical index of weathering. Sed Geol 55:319–322

Herron MM (1988) Geochemical classification of terrigenous sands and shales from core or log data. J Sediment Petrol 85:820–829

Ingersoll RV, Bullard TF, Ford RL, Grimm JP, Pickle JD, Sares SW (1984) The effect of grain size on detrital modes: a test of the Gazzi-Dickinson point-counting method. J Sediment Petrol 54: 103–116

Junner NR, Hirst T (1946) The geology and hydrology of the Voltaian Basin. Memoir 8 Accra Gold Coast Geol Survey 8:51

Kalsbeek F, Frei R (2009) Geochemistry of Precambrian sedimentary rocks used to solve stratigraphic problems: an example from the Neoproterozoic volta Basin, Ghana. Precamb Res 176:65–76

Kalsbeek F, Frei R (2010) Geochemistry of Precambrian sedimentary rocks used to solve stratigraphical problems: an example from the Neoproterozoic Volta Basin, Ghana. Precamb Res 176:65–76

Kalsbeek F, Frei D, Affaton P (2008) Constraints on provenance, stratigraphic correlation and structural context of the Volta basin, Ghana, from detrital zircon geochronology: an Amazonian connection? J Sed Geol 212:86–95

Maynard JB (1992) Chemistry of modern soils as a guide to interpreting Precambrian paleosols. J Geol 100:279–289

McLennan SM, Taylor SR, McCulloch MT, Maynard JB (1990) Geochemical and Nd–Sr isotopic composition of deep-sea turbidites: crustal evolution and plate tectonic associations. Geochim Cosmochim Acta 54:2015–2050

McLennan S M, Hemming S, McDaniel D K, Hanson G N (1993) Geochemical approaches to sedimentation, provenance and tectonics. In: Johnsson M J, Basu A (eds.). Processes Controlling the Composition of Clastic Sediments. Geol Soc Ame Spec Paper 285:21–40.

Morton A C, Hallsworth C R, Wilkinson G C (1993) Evolution of sand provenance during Paleocene deposition in the Northern North Sea. In J. R. Parker (Ed.), Petroleum Geology of Northwest Europe, Proceedings of the 4th Conference London. Geol Soc, p 73–84

Nesbitt HW, Young GM (1982) Early Proterozoic climate and plate motions inferred from major elements chemistry of lutites. Nature 299: 715–717

Nesbitt HW, Markovics G, Price RC (1980) Chemical processes affecting alkalis and alkaline earths during continental weathering. Geochim Cosmochim Acta 44:1659–1666

Pettijohn FJ, Potter PE, Siever R (1972) Sand and Sandstones, New York, Springer-Verlag

Taylor SR, McLennan SM (1985) The continental crust: its composition and evolution. Blackwell Scientific, Oxford, p 312

Tortosa A, Palomares M, Arribas J (1991) Quartz grain types in Holocene deposits from the Spanish central system: some problems in provenance analysis, in Morton A C, Todd S P, Haughton P D W (eds.) Developments in Sedimentary Provenance Studies,. Geol Soc Lond Spec Publ, 57:47–54

Verma SP, Armstrong-Altrin JS (2013) New multi-dimensional diagrams for tectonic discrimination of siliciclastic sediments and their application to Precambrian basins. Chem Geol 355:117–133

Verma SP, Armstrong-Altrin JS (2016) Geochemical discrimination of siliciclastic sediments from active and passive margin settings. Sed Geol 332:1–12

Viljeon J H A, Agyapong W, Le Berre W, Reddering J S V, Thomas E, Atta–Ntim K (2008) Geology of sheet 1001D south of Gambaga, Ghana